*plants*

MDPI

*Article*

# *Rhizoctonia solani* AG-4 HGI and *Agroathelia rolfsii* Causing Damping-Off and Southern Blight of Industrial Hemp in Yunnan, China, and Cross-Infection of *Ag. rolfsii* on Industrial Hemp and *Amorphophallus muelleri*

**Jian-Wei Guo [1], Min Yang [1], Murad Muhammad [2,3], Lifang Li [1], Penghua Gao [1], Yongteng Zhao [1], Ying Qi [1], Shaowu Yang [1], Lei Yu [1,*] and Chui-Si Kong [4,*]**

[1] College of Agronomy and Life Sciences, Yunnan Key Laboratory of Konjac Biology, Yunnan Urban Agricultural Engineering and Technological Research Center, Kunming University, Kunming 650214, China; gjwkf475001@sina.com (J.-W.G.); yangmin7799@163.com (M.Y.); csqsmile@126.com (L.L.); gaopenghua8878@dingtalk.com (P.G.); yongtengzhao@163.com (Y.Z.); qiying0621@126.com (Y.Q.); yangshaowu910@126.com (S.Y.)
[2] State Key Laboratory of Desert and Oasis Ecology, Key Laboratory of Ecological Safety and Sustainable, Development in Arid Lands, Xinjiang Institute of Ecology and Geography, Chinese Academy of Sciences, Urumqi 830011, China; muradbotany1@uop.edu.pk
[3] University of Chinese Academy of Sciences, Beijing 100049, China
[4] Agricultural Environment and Resources, Yunnan Academy of Agriculture Sciences, Kunming 650200, China
* Correspondence: yulei0425@163.com (L.Y.); wwwkcs@126.com or kcs@yaas.org.cn (C.-S.K.); Tel.: +86-871-65223006 (L.Y.)

## Abstract

The necrotrophic fungi *Rhizoctonia solani* (anamorph of *Thanatephorus cucumeris*) and *Agroathelia rolfsii* (Syn. *Sclerotium rolfsii*, anamorph of *Athelia rolfsii*) are soil-borne pathogens with host ranges spanning several hundred plant species, including rice, maize, cotton and tomato, worldwide. Since June 2023, damping-off of seedlings and southern blight of adult plants have been detected on industrial hemp in Wuding County, Chuxiong Prefecture, Yunnan Province, China. Disease incidence reached 30% and 2.4%, respectively. Two isolates, CSB1 and CSB2-1, were identified as *R. solani* AG-4 HGI based on cultural characteristics and ITS-TEF-based phylogenetic analysis, and five isolates from industrial hemp and one isolate from *Amorphophallus muelleri* were characterized as *A. rolfsii* based on cultural characteristics combined with ITS-LSU-TEF-based phylogenetic analysis. This is the first report of *R. solani* AG-4 HGI causing damping-off and *Ag. rolfsii* causing southern blight of industrial hemp in Yunnan Province, China. All six *Ag. rolfsii* isolates (five from hemp and one from *Am. muelleri*) cross-infected industrial hemp and *Am. muelleri* under artificial inoculation. These results provide a basis for rapid diagnosis, screening chemical and biological fungicides, and resistance breeding in industrial hemp.

**Keywords:** industrial hemp; *Rhizoctonia solani*; *Agroathelia rolfsii*; cross-infection; phylogenetic analysis

Check for updates

Academic Editor: William Underwood

Received: 14 August 2026
Revised: 9 November 2026
Accepted: 15 November 2026
Published: 18 November 2026

**Copyright:** © 2026 by the authors. Licensee MDPI, Basel, Switzerland. This article is an open access article distributed under the terms and conditions of the Creative Commons Attribution (CC BY) license.

## 1. Introduction

Industrial hemp (*Cannabis sativa* L.) is widely cultivated in Yunnan, Shanxi, and Heilongjiang Provinces and other regions in China [1]. It is widely used in medicine, functional food, cosmetics, additives, textiles, and paper manufacturing because of its rich fibers and low cannabinol (<0.3%) [2–4]. As of 2020, the plantation area of industrial hemp, including

the main cultivated varieties Yunma 7, 8, and 10, was $1.33 \times 10^4$ ha in Yunnan Province, China [5,6].

To date, more than 20 viruses, including industrial hemp cryptic virus (IHCV), cucumber mosaic virus (CMV), potato virus Y (PVY), and tobacco streak virus (TSV), have been reported to cause viral disease in *C. sativa* [1]. For fungal disease, crown and root rot caused by *Pythium aphanidermatum* has been found in Arizona, Indiana, USA [7,8] and Shandong, China [9], that caused by *P. ultimum* has been discovered in Indiana, USA [10], that caused by *P. myriotylum* has been reported in Massachusetts and Arizona, USA [11–13]; white root rot caused by *Dematophora necatrix* in Naples, Italy [14]; wilt (whole plant decline and root rot) caused by *Fusarium falciforme* in California, USA [15] and *F. oxysporum* in Heilongjiang, China has also been reported [16]; damping-off caused by *Rhizoctonia solani* has been found in Iraq [17], damping-off and seedling rot caused by *F. solani* have been discovered in North Dakota, USA [18]; southern blight with disease incidence of 10–50% caused by *Athelia rolfsii* (the teleomorph of *Agroathelia rolfsii*, syn. *Sclerotium rolfsii*) has been reported in Louisiana, USA [19], and stem canker with disease incidence of 30% caused by *Sclerotinia sclerotiorum* has been reported in California, USA [20]. In addition, leaf spot caused by *Alternaria alternata* in Heilongjiang, China [21] and *Cercospora* cf. *flagellaris* in Arkansas and Oklahoma, USA [22], as well as powdery mildew caused by *Golovinomyces ambrosiae* in New Jersey, USA [23] have been reported. Crown root rot caused by *P. aphanidermatum*, *P. ultimum*, and *P. myriotylum*, white root rot caused by *D. necatrix*, wilt caused by *Fusarium* spp., damping-off caused by *R. solani*, and southern blight caused by *S. rolfsii* on industrial hemp can cause death of the whole plant. Among them, southern blight caused by *A. rolfsii* first appeared as foliar yellowing and wilt, followed by necrosis at the stem base with white dense mycelium and reddish to dark brown sclerotia, which expanded into the root zone and onto the soil surface around the infected plants, finally the diseased plants turned brown and died [19]. Both diseases often show similar symptoms: water soaked, brown lesions on the stem base in the early stages, followed by sclerotia with disease progresses [24,25]. However, southern blight caused by *A. rolfsii* can infect host plants at different growth stages [26], while damping-off caused by *R. solani* usually shows symptoms at pre- or post-germination and results in shrunk stem base and mortality without collapse of seedlings [17,24]. Moreover, the mycelium of *A. rolfsii is* denser than that of *R. solani* on artificial media [27] or infected plants [28,29].

Additionally, *R. solani* (teleomorph: *Thanatephorus cucumeris*) is a soil-borne fungal pathogen that causes seed decay, root rot, damping-off, crown-stem canker, fruit rot, leaf blight, and sheath blight of cultivated crops, wild plants, and horticultural crops belonging to 263 species in 43 families [30–32]. Although cultural characteristics, biological and chemical characteristics, and pathogenicity differ clearly among strains of *R. solani*, those characteristics combined with sclerotial size, color, and structure are not sufficient to identify a separate species, which is thought to be a species complex and classified into different subgroups called anastomosis groups (AGs) based on hyphal anastomosis reactions [33,34]. Additionally, it is classed into 14 anastomosis groups [35,36]. Currently, ITS or TEF has been proposed to differentiate different anastomosis groups of *R. solani* [31]. *A. rolfsii* is also a globally distributed soil-borne fungal pathogen that can infect many plants belonging to more than 600 species of over 100 families; thus, it is one of the most economically important pathogens affecting wheat, soybean, peanut, sunflower, sesame, tomato, and so on [37]. Phylogenetic analysis based on ITS, LSU, or TEF sequence data is more frequently used to identify *Agroathelia* species than morphological characteristics [38–41].

However, comprehensive studies on fungal diseases of industrial hemp, including diversity, occurrence, and pathogenicity remain limited. Considering that *A. rolfsii* and *R. solani* can infect many crops including industrial hemp, and that large areas of industrial

hemp and konjac (collective term for *Amorphophallus* species) are cultivated in Chuxiong, Yunnan, China, the present study had three objectives. The first was to identify the causal pathogens of damping-off and southern blight on industrial hemp in Wuding County, Yunnan Province, China. The second was to confirm the isolates' pathogenicity on industrial hemp by artificial inoculation, in accordance with Koch's postulates. The third was to determine whether *Ag. rolfsii* can cross-infect industrial hemp and *Am. muelleri*.

## 2. Results

### *2.1. Natural Symptoms and Fungal Isolation of Damping-Off and Southern Blight*

The seedlings and plants of industrial hemp variety Yunma 8 (a multiple-purpose variety for seed, fiber, leaf, and bran) were commercially cultivated in the field. At the sample site, the soil was classified as red earth, well-drained, with a mean pH value of 6.0. *Amorphophallus muelleri* plants were cultivated in a greenhouse to breed varieties resistant to soft rot disease, and the soil was also classified as red earth, well-drained, with a pH range of 6.0–7.0. In early June 2023, an incidence of damping-off of about 30% among 1000 one-month-old seedlings was recorded in a plantation in Wuding County, Chuxiong Yi Autonomous Prefecture (Chuxiong Prefecture), Yunnan Province, China. Initially, the upper leaves turned yellowish and gradually withered; the stem base appeared water-soaked, then turned brown and shrank, finally, the whole plant withered. On rainy days, a layer of white and dense mycelia covered the stems of diseased seedlings (Figure 1A). In early August 2023, an incidence rate of southern blight was 2.4%, with white, thick and dense mycelia on the stem bases recorded among about 10,000 two-month-old adult plants (50,000 plants/ha) in the same plantation above. Initially, the stem base appeared white, with sparse mycelia and turned water-soaked; subsequently, the stem bases were covered with a layer of dense, leathery, and white mycelia and turned gray-white to brown; the roots developed brown rot, and the root bark was prone to shedding; finally, the whole plants withered and produced many yellowish to yellowish-brown sclerotia (Figure 1B). Meanwhile, a similar symptom was observed only at the petiole bases of *Am. muelleri* 13B-2-17 in Kunming City, Yunnan Province, China (Figure 1(C1–C3)), whereas the tubers were asymptomatic.

A total of two isolates, namely CSB1 and CSB2-1, were obtained from two diseased stems of damping-off on industrial hemp, five isolates were isolated from five diseased stems of southern blight on industrial hemp (namely CS1~CS5), and one isolate was isolated from one symptomatic petiole on *Am. muelleri* (namely AM1).

### *2.2. Morphological and Molecular Identification of Rhizoctonia solani* AG-4 HGI *and Agroathelia rolfsii*

The CSB1 and CSB2-1 colonies on PDA at 28 °C were initially white and sparse, then gradually turned brown. After 4 days, brown mycelial clusters gradually appeared on the surface, forming a clear radial pattern, and the colony diameter reached 8.0 cm. Additionally, after 14 days, sparse sclerotia were produced at the margin of the colonies of CSB1 and CSB2-1 (Figure 2A,B). These cultural characteristics were similar to those of *Rhizoctonia* spp. described by Basbagci and Dolar [42]. The colonies of CS1-CS5 and AM1 on PDA at 28 °C were circular and cotton-like, with white, dense mycelium and radiating growth; after 5–7 days of cultivation, the colonies reached 9.0 cm and the color gradually turned milky white; after 10–15 days of cultivation, the surface of the colony began to form sclerotia, initially appearing as small white spherical structures, gradually turning yellow-brown to dark brown. The sclerotia were spherical, smooth, and hard, with an individual diameter of 0.8–1.5 mm (Figure 2C–E). These cultural characteristics matched Tanjila et al.'s description of *Sclerotium* [43].

The ITS sequences of the isolates CSB1 (PZ832406) and CSB2-1 (PZ832407) showed 100% identity with the reference MN053034 of *R. solani* AG-4 SG_2T. In total, 39 isolates in the

present study comprised 1281 characters, including gaps (ITS: 1-717; TEF: 718-1281). The topologies resulting from ML and BI analyses of the concatenated dataset were congruent. In the ML/PP phylogenetic tree, the isolates CSB1 and CSB2-1 clustered in the branch consisting of *R. solani* AG4 SG_2T from rice, SG_732 from rice, AG-4 HGI BLS3 from potato, AG-4 HGI 433-16 from carrot, and AG4 HGI Chr-3 from *Chrysanthemum* x *morifolium* (Figure 3). Therefore, the isolates CSB1 and CSB2-1 were identified as *R. solani* AG4 HGI.




**Figure 1.** The natural symptoms of damping-off and southern blight on *Cannabis sativa* and *Amorphophallus muelleri*. (**A**) The natural symptoms of damping-off on one-month-old seedlings of *C. sativa*; (**B**) The natural symptoms of southern blight on adult plants of *C. sativa*; (**C1–C3**) The natural symptoms of southern blight on *Am. muelleri*.

The ITS and LSU sequences of the isolates CS1, CS2, CS3, CS4, CS5, and AM1 (ITS: PZ832400-PZ832405, LSU: PZ829855-PZ829860) showed 100% identity with the references PP134911 and PP112095 of *S. rolfsii* HGUP 20-10, respectively. The combined sequences of 24 isolates of *Athelia* species, one isolate of *Sclerotium* species, and one isolate of *Byssocorticium atrovirens* (32 isolates in total) consisted of 2142 characters, including gaps (ITS: 1-671; LSU: 672-1335; TEF: 1336-2142). Additionally, the topologies from ML and BI analyses of the concatenated dataset were consistent; in the ML/PP phylogenetic tree, isolates CS1, CS2, CS3, CS4, CS5, and AM1 clustered in a clade containing *Ag. rolfsii* HGUP 20-10 from *Allium tuberosum*, CCAS-BLM-1 from *Artocarpus heterophyllus*, YYBJ20 from pepper, MY17B-1 from *Am. mueller*, CBS745.84/AFTOL-ID 664 and 23_261 from *Alocasia* sp. (Figure 4). Therefore, the isolates CS1, CS2, CS3, CS4, CS5, and AM1 were identified as *Ag. rolfsii*.

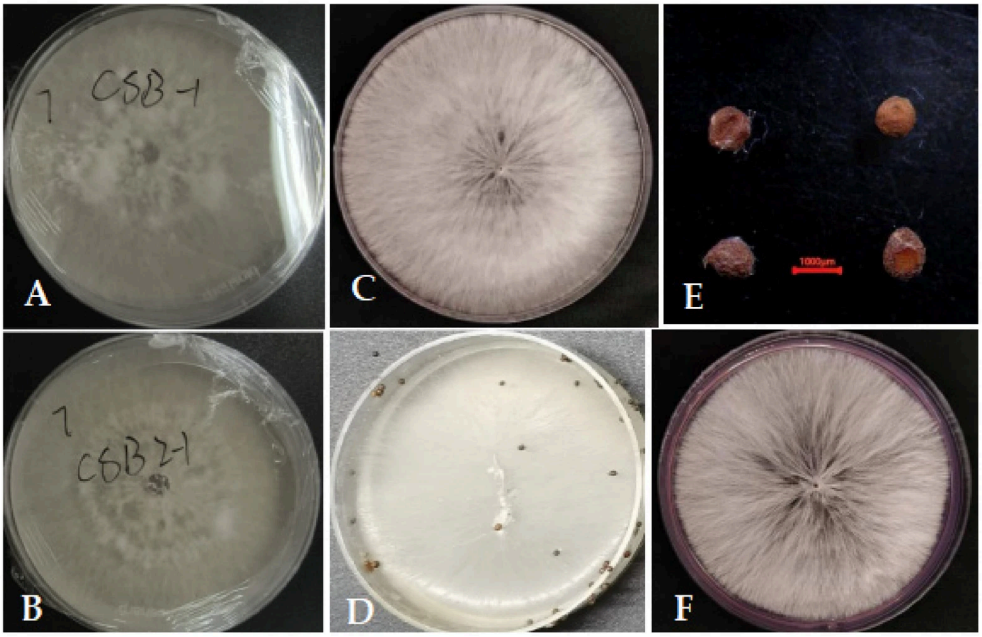



**Figure 2.** The cultural characteristics of *Rhizoctonia* and *Agroathelia*. (**A**) The front colony characteristics of *R. solani* CSB1 from industrial hemp on PDA; (**B**) The front colony characteristics of *R. solani* CSB2-1 from industrial hemp on PDA; (**C**) The front colony characteristics of *A. rolfsii* CS1 from industrial hemp on PDA; (**D**,**E**) The sclerotia of *S. rolfsii* CS1; (**F**) The front colony characteristics of *S. rolfsii* AM1 from *Amorphophallus muelleri* on PDA. (**E**) Bar = 1000 μm.

### *2.3. Pathogenicity Tests According to Koch's Postulates*

After 25 days of artificial inoculation with both isolates CSB1 and CSB2-1, the inoculated sites of industrial hemp developed water-soaked, brown necrotic lesions, then the top leaves of all inoculated seedlings turned yellowish, and the inoculated sites developed black rot after two months; finally, the whole seedlings wilted (Figure 5A–E). In contrast, the inoculated sites of the control plants only became dry. These symptoms were similar to the natural symptoms observed in the field, and the pathogen, identical to the previous isolates CSB1 and CSB2-1, was re-isolated from artificially inoculated plants to fulfill Koch's postulates.

To test the pathogenicity of five isolates (CS1–CS5) from industrial hemp and one isolate (AM1) from *Am. muelleri*, 5 mm mycelial plugs of each isolate were placed on the knife-wounded site of the stem or petiole base of ten industrial hemp plants and ten *Am. muelleri* plants. After 5 days of artificial infection, water-soaked symptoms appeared around the inoculated sites of industrial hemp, gradually, the diseased spots turned brown and were covered by a layer of white, dense mycelia. After three weeks, sclerotia formed at the base of all inoculated industrial hemp plants; finally, the whole plants wilted after two months (Figure 5F–H).

In contrast, the surrounding area of the inoculated sites of *Am. muelleri* inoculated by AM1 turned water-soaked and yellowish after five days of artificial infection; all the petioles with some sclerotia turned brown, shrank, and lodged; and the corresponding leaves withered after two weeks (Figure 5K,L), whereas the surrounding area of the inoculated sites of *Am. muelleri* inoculated by CS1, CS2, CS3, CS4, and CS5 from industrial hemp remained green, but the leaves turned yellowish after five days of artificial infection; all petioles with some sclerotia turned yellowish, shrank, lodged, and the corresponding leaves withered after two weeks (Figure 5I,J). All control plants were asymptomatic, with leaves and petioles remaining green (Figure 5M). Additionally, twenty isolates of the pathogen identical to the previous isolates were re-isolated from six symptomatic plants of industrial hemp and *Am. muelleri*, and the pathogenicity tests were repeated twice to fulfill Koch's postulates.

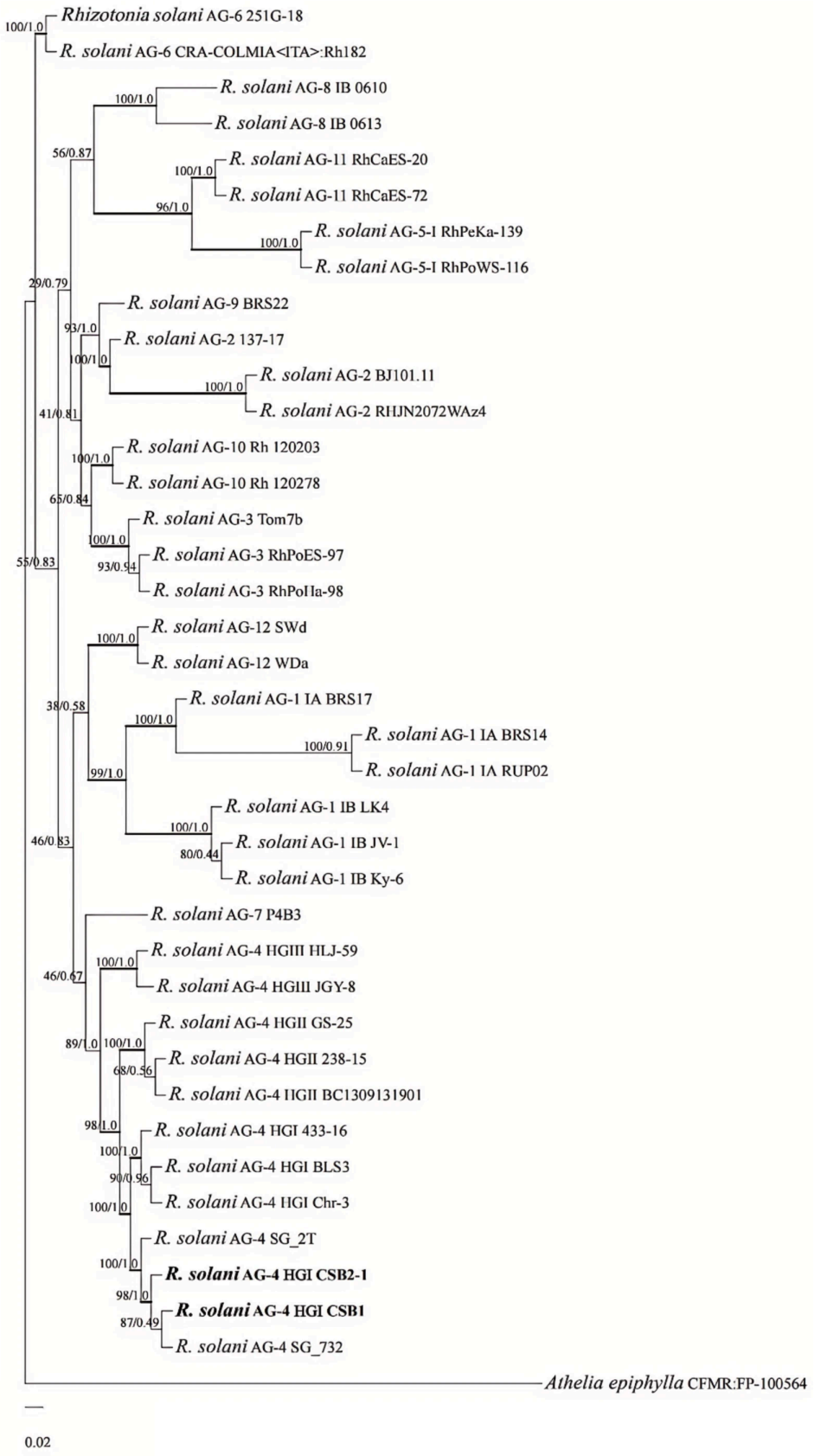



**Figure 3.** Phylogenetic tree derived from maximum likelihood analysis of 53 sequences of the combined ITS, TEF genes. All bootstrap values and Bayesian posterior probabilities are shown above the branches. Sequences of fungal strains obtained in this study are in bold. The scale bar shows the number of expected changes per site.

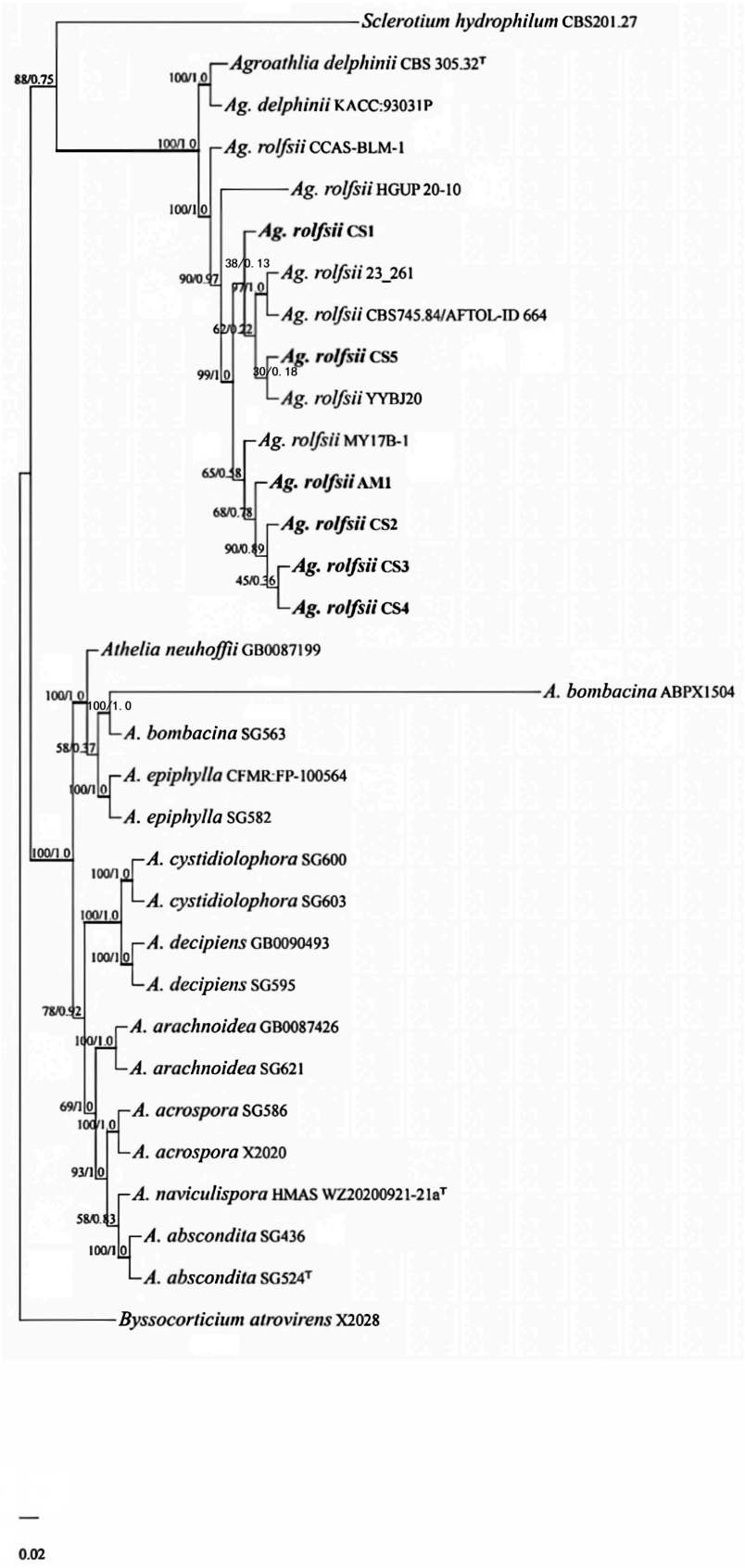



**Figure 4.** Phylogenetic tree derived from maximum likelihood analysis of 76 sequences of the combined ITS, LSU, and TEF genes. All bootstrap values and Bayesian posterior probabilities are shown above the branches. Sequences of fungal strains obtained in this study are in bold. The scale bar shows the number of expected changes per site.




**Figure 5.** The artificial infectious symptoms of industrial hemp and *Amorphophallus muelleri* cauded by *Rhizoctonia solani* and *Agroathelia rolfsii*. (**A**) The symptom of damping-off on industrial hemp inoculated by *R. solani* CSB1 after 25 days; (**B**–**D**) the symptom of damping-off on industrial hemp inoculated by *R. solani* CSB1 after two months; (**E**) the symptom of damping-off on industrial hemp inoculated by *R. solani* CSB2-1 after two months; (**F**–**H**) the symptom of southern blight on industrial hemp inoculated by *Ag. rolfsii* CS1, CS2 and AM1 after two weeks, respectively; (**I**,**J**) the symptom of southern blight on *Am. muelleri* inoculated by *Ag. rolfsii* CS1 after five days and two weeks, respectively; (**K**,**L**) the symptom of southern blight on *Am. muelleri* inoculated by *Ag. rolfsii* AM1 after five days and two weeks, respectively; (**M**) the control plants of *Am. muelleri* inoculated with 5 mm agar plugs after two weeks.

## 3. Discussion

Chuxiong Yi Autonomous Prefecture (Chuxiong Prefecture) is located in northern Yunnan Province, China [44]. The vegetable planting area in Chuxiong Prefecture is

$1.08 \times 10^4$ ha, and the konjac (collective term for *Amorphophallus* species, mainly including *Am. muelleri*, *Am. bulbifer*, *Am. konjac* and *Am. albus*) planting area is $1.33 \times 10^4$ ha. Additionally, the industrial hemp planting area is 533.33 ha in Wuding County, Chuxiong Prefecture. Accurate identification of disease symptoms and their corresponding pathogens underpin the development of colloidal-gold immunochromatographic assays, targeted disease control, resistance breeding, conservation biology, and ecosystem management [45–47]. Considering that *R. solani* can infect 263 host plant species of 43 families [30–32] and *A. rolfsii* can infect over 600 host plant species of more than 100 families [37], it is essential to establish the taxonomic status of the pathogens of damping-off and southern blight on industrial hemp in Wuding County, Chuxiong Prefecture, Yunnan Province, China.

Two isolates, CSB1 and CSB2-1, were identified as *R. solani* AG-4 HGI based on cultural characteristics and ITS phylogeny. *R. solani* AG-4 HGI and binucleate *Rhizoctonia* AGA have been reported to be agents of damping-off of Swiss chard (*Beta vulgaris* subsp. *cicla* L.) in Yunnan [48]. Binucleate *Rhizoctonia* anastomosis groups (AG) AG-P and AG-R, and *R. solani* AG-1 IB and AG-4 HGI have also been reported as pathogens causing wirestem of *Betula nigra* in Yunnan Province, China [49]. To our knowledge, this is the first report of *R. solani* AG-4 HGI causing damping-off on industrial hemp in Yunnan Province, China. However, further work is required to establish how many anastomosis groups can infect industrial hemp and the vegetable and other crops grown alongside it, and which group is dominant in Wuding County, Yunnan Province, China.

Five isolates from industrial hemp and one isolate from *Am. muelleri* were characterized as *Agroathelia rolfsii* (syn. *Sclerotium rolfsii*; teleomorph *Athelia rolfsii*) based on cultural characteristics combined with phylogenic analysis of concatenated ITS-LSU aligned combined sequences. *A. rolfsii* causing southern blight on industrial hemp with disease incidence of 10–50% has been reported in Louisiana, USA [19]; *S. sclerotiorum* causing stem canker on industrial hemp with a disease incidence of 30% has been reported in California, USA [20]. Moreover, *A. rolfsii* has been identified as the agent of southern blight disease of *Am. muelleri* in Mile City, Honghe Prefecture, Yunnan Province, China [50]. Thus, this is the first report of *A. rolfsii* causing southern blight on industrial hemp in Yunnan Province, China, and the first report of cross-infection by *A. rolfsii* between industrial hemp and *Am. muelleri*. These findings indicate that intercropping, interplanting, and crop rotation between industrial hemp and *Am. muelleri* should be avoided.

## 4. Materials and Methods

### *4.1. Field Symptom Observation and Fungal Isolation*

In early June 2023, damping-off was observed in one-month-old industrial hemp seedlings in Wuding County, Chuxiong Prefecture, Yunnan Province, China, and the incidence was then surveyed in 1000 seedlings. Twenty-two diseased seedlings from five pots were taken to the laboratory for fungal isolation. In early August 2023, southern blight was also discovered on two-month-old plants, and its incidence was assessed in about 10,000 plants; meanwhile, southern blight on two-year-old plants of *Am. muelleri* was found in Kunming City, Yunnan Province, China, and its incidence was evaluated on about 6000 plants. Five diseased hemp plants and one *Am. muelleri* plant were dug up and taken to the laboratory for fungal isolation.

Three living diseased seedlings were surface-sterilized with 5% sodium hypochlorite for 3 min, washed 5 times with sterilized water; the diseased tissues were cut into 0.5 cm × 0.5 cm pieces and transferred to rose bengal agar (RBA) at 28 °C for five days, after which the germinated hyphal tips were picked onto potato dextrose agar (PDA) following the description by Guo et al. [46,51]. Mycelia from five industrial hemp plants and one *Am.*

*muelleri* plant with southern blight were picked and transferred to RBA at 28 °C for two days, then the freshly germinated hyphal tips were picked onto PDA.

### *4.2. Morphological and Molecular Identification of Rhizoctonia and Agroathelia*

The 5 mm mycelial plugs were transferred onto PDA at 28 °C to assess mycelial growth and sclerotia production; the shape and size of sclerotia ($n = 30$) were photographed and measured using an Olympus SZ51 microscope (Olympus, Tokyo, Japan).

The genomic DNA of each isolate was extracted from mycelium grown on PDA plates at 28 °C for seven days using a Solarbio Fungi Genomic DNA Extraction Kit (Beijing Solarbio Science & Technology Co., Ltd., Beijing, China) following the manufacturer's protocol. The PCR reaction volume and PCR parameters followed by the description by Guo et al. [46]. The internal transcribed spacer (ITS) regions of all eight isolates were amplified and sequenced using the primers ITS1/ITS4, and the LSU regions of six *Agroathelia* isolates were amplified and sequenced using the primers LR0R/LR5 [46]. Finally, the amplified PCR products were sequenced by Tsingke Biotechnology Co., Ltd., Beijing, China.

For phylogenetic analysis, the 36 ITS sequences of 36 isolates belonging to 13 AGs of *R. solani*, and the TEF sequences of 13 isolates among the 36 isolates belonging to 6 AGs were downloaded. *A. epiphylla* (the teleomorph of *R. carotae*, GU187501 for ITS and GU187676 for TEF) was used as the outgroup for *R. solani*. The ITS, LSU, and TEF sequences belonging to 24 isolates of 10 *Athelia* species and one *Sclerotium* species (teleomorph not yet found), were first downloaded, and *Byssocorticium atrovirens* (LR694198 for ITS, LR694175 for LSU, and LR694214 for TEF) was used as the outgroup for *Athelia* species. Tables 1 and 2 list the GenBank accession numbers for the sequences used in the phylogenetic analyses. Then, the sequences of two or three loci were aligned and concatenated before manual refinement using BioEdit v. 7.0.4.1 [52], and ambiguously aligned sections were subsequently removed. The combined sequences were converted to NEXUS (for Bayesian inference analysis) and PHYLIP (for maximum likelihood analysis) files using ALTER [53], respectively.

**Table 1.** *Rhizoctonia solani* sequences in this study along with *Athelia epiphylla* data from GenBank.

| Specific Name | Isolate Number | Host | Location | GenBank Accession Numbers | |
|---|---|---|---|---|---|
| | | | | ITS | TEF |
| *Rhizoctonia solani* AG-1 IA | BRS14 | Unknown | Telangana, India | MK480532 | NA |
| *R. solani* AG-1 IA | RUP02 | Rice | Peninsular, Malaysia | KX674518 | KX674539 |
| *R. solani* AG-1 IA | BRS17 | Rice | Telangana, India | MK481078 | MN078941 |
| *R. solani* AG-1 IB | Ky-6 | *Cynanchum paniculatum* | Shandong, China | JQ343831 | NA |
| *R. solani* AG-1 IB | LK4 | Tobacco | Guizhou, China | MN749891 | NA |
| *R. solani* AG-1 IB | JV-1 | *Mentha longifolia* | Israel | JN254787 | NA |
| *R. solani* AG-2 | BJ101.11 | *Bletilla striata* | Guangxi, China | MT892815 | NA |
| *R. solani* AG-2 | 137-17 | Pepper | Serbia | MN961109 | MT063198 |
| *R. solani* AG-2 | RHJN2072WAz4 | Azalea | Mississippi, USA | HQ404662 | NA |
| *R. solani* AG-3 | RhPoHa-98 | Potato | Gotland, Sweden | MW999201 | NA |
| *R. solani* AG-3 | RhPoES-97 | Potato | Scania, Sweden | MW999200 | NA |
| *R. solani* AG-3 | Tom7b | Tomato | North Carolina, USA | GQ885147 | LC274631 |
| *R. solani* AG-4 | SG_732 | Rice | Texas, USA | MN053033 | NA |
| *R. solani* AG-4 | SG_2T | Rice | Texas, USA | MN053034 | NA |
| ***R. solaniHGI* AG-4 HGI** | **CSB1** | **Industrial hemp** | **Yunnan, China** | **PZ832406** | **NA** |
| ***R. solaniHGI* AG-4 HGI** | **CSB2-1** | **Industrial hemp** | **Yunnan, China** | **PZ832407** | **NA** |
| *R. solani* AG-4 HGI | BLS3 | Potato | Maseru, Lesotho | PV167481 | PV449100 |
| *R. solani* AG-4 HGI | 433-16 | Carrot | Serbia | MN961154 | MT063203 |
| *R. solani* AG-4 HGI | Chr-3 | *Chrysanthemum* x *morifolium* | Japan | AB000015 | LC274659 |
| *R. solani* AG-4 HGII | GS-25 | Potato | Gansu, China | JX843820 | NA |
| *R. solani* AG-4 HGII | 238-15 | Apple | Serbia | MN966409 | MT063199 |
| *R. solani* AG-4 HGII | BC1309131901 | Unknown | China | MH483967 | MH938394 |
| *R. solani* AG-4 HGIII | HLJ-59 | Sugar beet | China | MH172666 | NA |
| *R. solani* AG-4 HGIII | JGY-8 | Potato | China | KJ866417 | KJ866454 |
| *R. solani* AG-5-I | RhPeKa-139 | Pea | Sweden | OP890582 | PX829085 |
| *R. solani* AG-5-I | RhPoWS-116 | Potato | Scania, Sweden | MW999202 | PX829090 |

**Table 1.** *Cont.*

| Specific Name | Isolate Number | Host | Location | GenBank Accession Numbers | |
|---|---|---|---|---|---|
| | | | | ITS | TEF |
| *R. solani* AG-6 | 251G-18 | Raspberry | Serbia | MN961149 | MT063200 |
| *R. solani* AG-6 | CRA-COLMIA<ITA>:Rh182 | Apple rootstock M9 | South Tyrol, Italy | JF519844 | NA |
| *R. solani* AG-7 | P4B3 | *Gossypium hirsutum* | Pella, Greece | FJ480892 | NA |
| *R. solani* AG-8 IB | 0613 | Wheat | Turkey | KC590586 | NA |
| *R. solani* AG-8 IB | 0610 | Wheat | Turkey | KC590583 | NA |
| *R. solani* AG-9 | BRS22 | Rice | India | MK483716 | NA |
| *R. solani* AG-10 | Rh 120203 | Wheat | Washington, USA | DQ356410 | NA |
| *R. solani* AG-10 | Rh 120278 | Chickpea | Washington, USA | DQ356408 | NA |
| *R. solani* AG-11 | RhCaES-72 | Carrot | Scania, Sweden | MW999184 | NA |
| *R. solani* AG-11 | RhCaES-20 | Carrot | Scania, Sweden | MW999183 | NA |
| *R. solani* AG-12 | WDa | Unknown | Sydney, Australia | AF153807 | NA |
| *R. solani* AG-12 | SWd | Unknown | Sydney, Australia | AF153806 | NA |
| *Athelia epiphylla* (the teleomorph of *R. carotae*) | CFMR:FP-100564 | Unknown | Maryland, USA | GU187501 | GU187676 |

Note: Strains in this study are in bold; ex-type strains are denoted with superscript T; and NA indicates data unavailability.

**Table 2.** *Athelia* sequences in this study along with additional *Byssocorticium atrovirens* data from GenBank.

| Specific Name | Isolate Number | Host | Location | GenBank | | |
|---|---|---|---|---|---|---|
| | | | | ITS | LSU | TEF1 |
| *Athelia abscondita* | SG524$^{T}$ | *Bryoria* sect. Implexae | Montana, USA | OP877120 | OP902328 | OQ446120 |
| *A. abscondita* | SG436 | *Usnea* sp. | Alberta, Canada | OP877102 | OP902312 | OQ446113 |
| *A. acrospora* | SG586 | *Picea engelmanni* | Washington, USA | OP877141 | OP902347 | NA |
| *A. acrospora* | X2020 | Unkown | Norway | MT305993 | MT305993 | LR794095 |
| *A. arachnoidea* | SG621 | *Bryoria* sp. | Kainbach bei Voitsberg, Austria | OP877154 | OP902360 | NA |
| *A. arachnoidea* | GB0087426 | Unkown | Sweden | LR694192 | LR694169 | LR694213 |
| *A. bombacina* | ABPX1504 | Korla Xiang pear | Hebei, China | KX610836 | KX610837 | NA |
| *A. bombacina* | SG563 | Pine | Alberta, Canada | OP877133 | OP902340 | NA |
| *A. cystidiolophora* | SG600 | *Pinus sylvestris* | Vazhinka, Russia | OP877148 | OP902354 | NA |
| *A. cystidiolophora* | SG603 | *Quercus robus* | Krastelikha, Russia | OP877150 | OP902356 | NA |
| *A. decipiens* | GB0090493 | Unkown | Sweden | LR694193 | LR694170 | NA |
| *A. decipiens* | SG595 | *Pinus sylvestris* | Chagoda, Russia | OP877145 | OP902351 | OQ446104 |
| *A. epiphylla* | SG582 | *Picea glauca* | Alberta, Canada | OP877140 | OP902346 | OQ446103 |
| *A. epiphylla* | CFMR:FP-100564 | Unknown | Maryland, USA | GU187501 | GU187558 | GU187676 |
| *A. naviculispora* | HMAS WZ20200921-21a$^{T}$ | Unkown | USA | NR_197530 | NG_243387 | NA |
| *A. neuhoffii* | GB0087199 | Unkown | Sweden | LR694195 | OP902351 | NA |
| *Agroathelia delphinii* | CBS 305.32$^{T}$ | Unkown | USA | NR_189755 | NG_241907 | NA |
| *Ag. delphinii* | KACC:93031P | Unkown | South Korea | OR981825 | PQ357635 | PQ408028 |
| *Ag. rolfsii* | HGUP 20-10 | *Allium tuberosum* | Guizhou, China | PP134911 | PP112095 | NA |
| *Ag. rolfsii* | CCAS-BLM-1 | *Artocarpus heterophyllus* | Guangdong, China | OP535473 | OP535474 | NA |
| *Ag. rolfsii* | YYBJ20 | Pepper | Hunan, China | OQ186649 | NA | OQ221158 |
| *Ag. rolfsii* | MY17B-1 | *Amorphophallus mueller* | Yunnan, China | OP658949 | OP658955 | OP679794 |
| *Ag. rolfsii* | CBS745.84/AFTOL-ID 664 | Unkown | USA | DQ484062 | AY635773 | GU187681 |
| *Ag. rolfsii* | 23_261 | *Alocasia* sp. | Florida, USA | PQ436344 | PQ428904 | PQ441996 |
| ***Ag. rolfsii*** | **CS1** | **Industrial hemp** | **Yunnan, China** | **PZ832400** | **PZ829855** | **NA** |
| ***Ag. rolfsii*** | **CS2** | **Industrial hemp** | **Yunnan, China** | **PZ832401** | **PZ829856** | **NA** |
| ***Ag. rolfsii*** | **CS3** | **Industrial hemp** | **Yunnan, China** | **PZ832402** | **PZ829857** | **NA** |
| ***Ag. rolfsii*** | **CS4** | **Industrial hemp** | **Yunnan, China** | **PZ832403** | **PZ829858** | **NA** |
| ***Ag. rolfsii*** | **CS5** | **Industrial hemp** | **Yunnan, China** | **PZ832404** | **PZ829859** | **NA** |
| ***Ag. rolfsii*** | **AM1** | ***Ammorphophallus mueller*** | **Yunnan, China** | **PZ832405** | **PZ829860** | **NA** |
| *Sclerotium hydrophilum* | CBS201.27 | Unknown | Netherlands | FJ231396 | MH866422 | NA |
| *Byssocorticium atrovirens* | X2028 | Unknown | Sweden | LR694198 | LR694175 | LR694214 |

Note: Strains in this study are in bold; ex-type strains are denoted with superscript T; and NA indicates data unavailability.

To confirm the phylogenetic relationship of *R. solani* CSB1 and CSB2-1, a multigene maximum likelihood (ML) phylogenetic analysis was performed in IQ-TREE 2.4.0 (https://iqtree.github.io/). ModelFinder selected partition-specific models using the Bayesian Information Criterion (BIC), with the best-fit models of nucleotide substitution being HKY + F + R2:ITS and TNe + I + G4: TEF. SH-aLRT and UFBoot bootstrap analyses were run with 1000 replicates, respectively. Bayesian inference (BI) was run in MrBayes v. 3.2.7a [54] using partitioned GTR + Gamma models. Markov Chain Monte Carlo (MCMC) of four simultaneous Markov chains were run for 0.3 million generations to determine posterior probabilities (PP), and the first 25% of trees, representing the burn-in phase, were discarded before the majority-rule consensus tree was built. The final average standard deviation of split frequencies (ASDSF) was 0.010362. Alignments derived from this study were deposited in TreeBASE (submissiona ID S32835). The phylogram was visualized in FigTree v. 1.4.0 [55] and edited in Microsoft Office PowerPoint 2019 (Microsoft Inc., Redmond, WA, USA).

Similarly, a ML phylogenetic analysis of CS1, CS2, CS3, CS4, CS5, and AM1 was also carried out in IQ-TREE 2.4.0 (https://iqtree.github.io/). ModelFinder selected partition-specific models using BIC, with the best-fit nucleotide substitution models being TN + F + G4: ITS, TN + F + G4: LSU, and TN + G4: TEF. At the same time, the average standard deviation of split frequencies (ASDSF) was 0.013098. Alignments derived from this study were deposited in TreeBASE (submission ID S32835). Other processes followed the methods above.

### *4.3. Pathogenicity Determination of Rhizoctonia and Agroathelia*

To test the pathogenicity of CSB1 and CSB2-1 from industrial hemp, ten 5 mm mycelial plugs of each isolate were placed upside down on wounded stem base surfaces of ten healthy one-month-old seedlings, respectively [46].

To determine the pathogenicity of CS1, CS2, CS3, CS4, and CS5 from industrial hemp and AM1 from *Am. muelleri*, the 5 mm mycelial plugs of each were inoculated on healthy one-month-old seedlings of industrial hemp and healthy two-year-old plants of *Am. muelleri* according to the methods above, respectively, and each treatment was replicated ten times [46].

Meanwhile, twenty 5 mm agar plugs were inoculated onto wounded stem base surfaces of ten healthy one-month-old industrial hemp seedlings and wounded petiole base surfaces of ten healthy two-year-old *Am. muelleri* as control plants, respectively. All the inoculated sites were first covered by a layer of absorbent cotton, and then a layer of tinfoil to maintain humidity. Additionally, we supplemented all inoculated sites with 3 mL of sterilized water daily for 5 days [46,51].

After the inoculated plants became symptomatic, the diseased stems or petioles were collected to re-isolate the pathogen as described in Section 4.1.

## 5. Conclusions

This study identified *Rhizoctonia solani* AG-4 as the causal agent of damping-off and *Agroathelia rolfsii* as the causal agent of southern blight of industrial hemp in Wuding County, Yunnan Province, China, based on cultural characteristics, ITS- or ITS-LSU-based phylogenies, and pathogenicity tests fulfilling Koch's postulates. This is the first report of *R. solani* AG-4 causing damping-off and *A. rolfsii* causing southern blight of industrial hemp in Yunnan Province, China. Cross-inoculation further showed that all six *A. rolfsii* isolates were pathogenic to both industrial hemp and *Am. muelleri*, indicating that the two crops can share an inoculum source in this production area. Whether *R. solani* AG-4 HGI can also infect *Am. muelleri* was not tested here and remains to be determined. Pending that evidence, intercropping, interplanting, and rotation between industrial hemp and *Am.*

*muelleri* should be avoided, and sclerotium-contaminated soil and crop residues should be treated as a carry-over inoculum reservoir. These results provide a basis for rapid diagnosis, for screening chemical and biological fungicides, and for resistance breeding in industrial hemp. Future work should quantify the anastomosis-group composition of *R. solani* across Yunnan's hemp-growing area and measure yield losses caused by both pathogens under field conditions.

**Author Contributions:** Conceptualization, L.Y. and J.-W.G.; Data curation, M.Y. and J.-W.G.; Formal analysis, L.L.; Funding acquisition, J.-W.G., L.Y. and C.-S.K.; Investigation, L.Y. and J.-W.G.; Methodology, M.Y. and J.-W.G.; Project administration, J.-W.G. and L.Y.; Software, M.Y., P.G., Y.Z., Y.Q. and S.Y.; Supervision, J.-W.G. and L.Y.; Validation, M.Y., P.G., Y.Z., Y.Q. and S.Y.; Visualization, J.-W.G.; Writing—original draft, J.-W.G.; Writing—review and editing, J.-W.G., M.M. and L.Y. All authors have read and agreed to the published version of the manuscript.

**Funding:** This research was funded by the Kunming University Talent Program (XJ20230077), the Yunnan Provincial Science and Technology Department (grant no. 202449CE340009, 202503AP140005, 202401BA070001-001), Yunnan Province Yu Lei Expert Grassroots Research Workstation, and the Yunnan Province Expert Workstation of Cai Peng (202405AF140079).

**Data Availability Statement:** The sequences of CS1, CS2, CS3, CS4, CS5, AM1, CSB1, and CSB2-1 (PZ832400-PZ832407 for ITS), as well as the sequences of CS1, CS2, CS3, CS4, CS5, and AM1 (PZ829855-PZ829860 for LSU) have been deposited in NCBI and made publicly available.

**Acknowledgments:** The authors would like to thank Qi Gao and Zheng-Yang Zhu for nursing the plants of industrial hemp and *Am. muelleri*. We also thank Shiyu Zhang for assistance in constructing phylogenetic trees.

**Conflicts of Interest:** The authors declare no conflicts of interest.

## References

1. Liu, Y.; Xu, Y.; Su, X.; Guan, F.; Zheng, K.; Chen, X. The genomic characteristics of a novel partitivirus infecting industrial hemp in Yunnan, China. *Microorganisms* **2025**, *13*, 2682. [CrossRef] [PubMed]
2. Rupasinghe, H.P.V.; Davis, A.; Kumar, S.K.; Murray, B.; Zheljazkov, V.D. Industrial hemp (*Cannabis sativa* subsp. *sativa*) as an emerging source for value-added functional food ingredients and nutraceuticals. *Molecules* **2020**, *25*, 4078. [CrossRef] [PubMed]
3. Schluttenhofer, C.; Yuan, L. Challenges towards revitalizing hemp: A multifaceted crop. *Trends Plant Sci.* **2017**, *22*, 917–929. [CrossRef] [PubMed]
4. Enarevba, D.R.; Haapala, K.R. The emerging hempindustry: A review of industrial hemp materials and product manufacturing. *AgriEngineering* **2024**, *6*, 2891–2925. [CrossRef]
5. Zhao, H.H.; Chen, J.K.; Xiong, H.P. Research on the innovative development strategies of industrial hemp seed industry in China. *Res. Agric. Mod.* **2020**, *41*, 765–771. [CrossRef]
6. Jiang, X.; Zhao, Y.X.; Teng, Y.J.; Li, X.L. Cannabinoids and terpenoids in hemp inflorescence and leaves of three varieties in Yunnan China. *Rapid Commun. Mass Spectrom.* **2026**, *40*, e70111. [CrossRef] [PubMed]
7. Hu, J.; Masson, R. First report of crown and root rot caused by *Pythium aphanidermatum* on industrial hemp (*Cannabis sativa*) in Arizona. *Plant Dis.* **2021**, *105*, 2257. [CrossRef]
8. Beckerman, J.; Nisonson, H.; Albright, N.; Creswell, T. First report of *Pythium aphanidermatum* crown and root rot of industrial hemp in the United States. *Plant Dis.* **2017**, *101*, 1038. [CrossRef]
9. Chen, J.; Li, Z.; Cheng, Y.; Gao, C.; Guo, L.; Wang, T.; Xu, J. First report of crown and root rot caused by *Pythium aphanidermatum* on industrial hemp (*Cannabis sativa*) in China. *Plant Dis.* **2022**, *106*, 1067. [CrossRef] [PubMed]
10. Beckerman, J.; Stone, J.; Ruhl, G.; Creswell, T. First report of *Pythium ultimum* crown and root rot of industrial hemp in the United States. *Plant Dis.* **2018**, *102*, 2045. [CrossRef]
11. McGehee, C.S.; Apicella, P.; Raudales, R.; Berkowitz, G.; Ma, Y.; Durocher, S.; Lubell, J. First report of root rot and wilt caused by *Pythium myriotylum* on hemp (*Cannabis sativa*) in the United States. *Plant Dis.* **2019**, *103*, 3288. [CrossRef]
12. Hu, J. First report of crown and root rot caused by *Pythium myriotylum* on hemp (*Cannabis sativa*) in Arizona. *Plant Dis.* **2021**, *105*, 2736. [CrossRef]
13. Brown, A.; Blit, E.; Gerstenberg, S.; Say, K.; Philbrook, R. First report of *Pythium myriotylum* causing damping off and root rot in *Cannabis sativa* in Florida. *Plant Dis.* **2026**, *110*, 1026. [CrossRef]

14. Sorrentino, R.; Baldi, G.M.; Battaglia, V.; Raimo, F.; Piccirillo, G.; Lahoz, E. First report of white root rot of hemp (*Cannabis sativa*) caused by *Dematophora necatrix* in Campania region (Southern Italy). *Plant Dis.* **2021**, *105*, 3299. [CrossRef]
15. Paugh, K.R.; Del Castillo Mu'nera, J.; Sweet, C.L. First report of *Fusarium falciforme* (FSSC 3+4) causing rot of industrial hemp (*Cannabis sativa*) in California. *Plant Dis.* **2022**, *106*, 1753. [CrossRef]
16. Tang, L.; Fan, C.; Guo, X.; Yuan, H.; Wu, G.; Zhang, S. First report of *Fusarium* wilt of industrial hemp (*Cannabis sativa*) caused by *Fusarium oxysporum* in Northeast China. *Plant Dis.* **2022**, *106*, 3205. [CrossRef]
17. Al-Beldawi, A.S.; Jawad, A.; Sheik-Raddy, H.M. *Rhizoctonia* seedling disease of hemp and its control. *Crop Prot.* **1982**, *1*, 111–113. [CrossRef]
18. Khan, M.F.R.; Bhuiyan, M.Z.R.; Lakshman, D.K.; Liu, Y.; Mosher, P.; Knoke, S. First report of damping-off and seedling rot of industrial hemp (*Cannabis sativa*) caused by *Fusarium solani* in North Dakota, U.S.A. *Plant Dis.* **2023**, *107*, 232. [CrossRef]
19. Singh, R.; De Sousz, M.; Burks, T.; Price, T. First report of southern blight of industrial help caused by *Athelia rolfsii* in Louisiana. *Plant Health Process* **2022**, *23*, 101–102. [CrossRef]
20. Yang, X.; Justice, A.; Colburn, G.C. First report of *Sclerotinia sclerotiorum* causing stem canker on industrial help in South California, U.S.A. *Plant Dis.* **2023**, *107*, 2870. [CrossRef]
21. Tang, L.; Song, X.; Zhang, L.; Wang, J.; Zhang, S. First report of leaf spot on industrial hemp (*Cannabis sativa*) caused by *Alternaria alternata* in China. *Plant Dis.* **2021**, *105*, 3294. [CrossRef]
22. Swift, K.B.; Bluhm, B.H. First report of *Cercospora* leaf spot caused by *Cercospora* cf. *flagellaris* on Industrial Hemp (*Cannabis sativa*) in Arkansas and Oklahoma. *Plant Dis.* **2025**, *109*, 1992. [CrossRef]
23. Rajmohan, N.; Price, D.C.; Buckley, R.J.; Komar, S.J.; Bamka, W.J.; Petit, E.A.; Cabrera, R.I.; Gianfagna, T.J.; Simon, J.E.; Wyenandt, C.A. First report of powdery mildew caused by *Golovinomyces ambrosiae* on industrial hemp in New Jersey. *Plant Dis.* **2022**, *106*, 2534. [CrossRef]
24. Lamichhane, J.A.; Dürr, C.; Schwanck, A.A.; Robin, M.H.; Sarthou, J.P.; Cellier, V.; Messéan, A.; Aubertot, J.N. Integrated management of damping-off diseases. A review. *Agron. Sustain. Dev.* **2017**, *37*, 10. [CrossRef]
25. Zhu, J.Z.; Ma, Y.M.; Wang, X.L.; Zhong, J.; Zhang, Z.; Li, X.G. First report of southern blight on *Aloe vera* caused by *Athelia rolfsii* in China. *Plant Dis.* **2022**, *106*, 2531. [CrossRef]
26. Ismaila, U.Y.; Okon, O.G.; Lovina, U.; Oluwaseu, D.A. Incidence and severity of vine rot and wilt disease of *Telfairia occidentalis* caused by *Athelia rolfii* in Southern, Nigeria. *Asian Plant Res. J.* **2024**, *12*, 22–31. [CrossRef]
27. Sri, B.N.; Sagar, B.V.; Padmaja, G.; Upendhar, S. Survey on soil-borne fungal diseases in chilli (*Capsicum annuum* L.) in Telangana State, India. *J. Adv. Biol. Biotechnol.* **2026**, *29*, 756–767. [CrossRef]
28. Godoy-Lutz, G.; Steadman, J.R.; Higgins, B.; Powers, K. Genetic variation among isolates of the web blight pathogen of common bean based on PCR-RFLP of the ITS-rDNA region. *Plant Dis.* **2003**, *87*, 766–771. [CrossRef] [PubMed]
29. Paparu, P.; Acur, A.; Kato, F.; Acam, C.; Nakibuule, J.; Nkuboye, A.; Musoke, S.; Mukankusi, C. Morphological and pathogenic characterization of *Sclerotium rolfsii*, the causal agent of southern blight disease on common bean in Uganda. *Plant Dis.* **2020**, *104*, 2130–2137. [CrossRef] [PubMed]
30. Rush, C.M. Prevalence and pathogenicity of anastomosis groups of *Rhizoctonia solani* from wheat and sugar beet in Texas. *Plant Dis.* **1994**, *78*, 349–352. [CrossRef]
31. Gurkanli, C.T.; Ozkoc, I.; Gunduz, I. Molecular and conventional identification and pathogenicity of *Rhizoctonia solani* isolates from tobacco (*Nicotiana tabacum* L.) in Samsun, Turkey. *J. Phytopathol.* **2009**, *157*, 686–696. [CrossRef]
32. Mishra, P.K. Phenotyping and cross infectivity of *Rhizoctonia solani* isolates originated from various hosts. *Trends Biosci.* **2015**, *8*, 6450–6454.
33. Yuvaraj, M.; Kannan, C.; Lokesh, R.; Ajaydesouza, V. Cultural and morpho-molecular characterization of *Rhizoctonia solani* causing rice sheath blight. *Biochem. Cell. Arch.* **2025**, *25*, 1007–1016. [CrossRef]
34. Carling, D.E.; Kuninaga, S.; Brainard, K.A. Hyphal anastomosis reactions, rDNA-internal transcribed spacer sequences, and virulence levels among subsets of *Rhizoctonia solani* anastomosis group-2(AG-2) and AG-BI. *Phytopathology* **2008**, *92*, 43–50. [CrossRef] [PubMed]
35. Priyatmojo, A.; Escopalao, V.E.; Tangonan, N.G.; Pascual, C.B.; Suga, H.; Kageyama, K.; Hyakumachi, M. Characterization of a new subgroup of *Rhizoctonia solani* anastomosis group 1 (AG-1-ID), causal agent of a necrotic leaf spot on coffee. *Phytopathology* **2001**, *91*, 1054–1061. [CrossRef] [PubMed]
36. Fiers, M.; Edel-Hermann, V.; Héraud, C.; Gautheron, N.; Chatot, C.; Le-Hingrat, Y.; Bouchek-Mechiche, K.; Steinberg, C. Genetic diversity of *Rhizoctonia solani* associated with potato tubers in France. *Mycologia* **2011**, *103*, 1230–1244. [CrossRef] [PubMed]
37. Xu, Z.; Gleason, M.L.; Mueller, D.S.; Esker, P.; Bradley, C.; Buck, J.W.; Benson, D.M.; Dixon, P.M.; Monteiro, J.E.P.A. Overwintering of *Sclerotium rolfsii* and *S. rolfsii* var. *delphinii* in different latitudes of the United States. *Plant Dis.* **2008**, *92*, 719–724. [CrossRef] [PubMed]
38. Pandey, M.K.; Sarma, B.K.; Singh, U.P. Induction of sexual stage and colony morphology of some isolates of *Sclerotium rolfsii* causing spotted leaf rot in plants. *Mycobiology* **2005**, *33*, 7–11. [CrossRef] [PubMed]

39. Nie, Q.; Zheng, T.; Liu, L.; Jiang, J.W.; Cheng, S.; Hsiang, T.; Sun, Z.X.; Zhou, Y. First report of southern blight on *Pinellia ternata* caused by *Athelia rolfsii* in China. *Plant Dis.* **2020**, *104*, 11. [CrossRef]
40. Kamil, D.; Bahadur, A.; Debna, T.H.P.; Kumari, A.; Choudhary, S.P.; Thokala, P. First report of leaf sheath rot of Areca nut (*Areca catechu*) caused by *Athelia rolfsii* from Tripura, India. *Plant Dis.* **2020**, *104*, 1–2. [CrossRef]
41. Seo, Y.; Park, M.J.; Back, C.G.; Park, J.H. First report of stem rot caused by *Athelia rolfsii* on *Zamioculcas zamiifolia* in Korea. *Plant Dis.* **2019**, *103*, 1–4. [CrossRef]
42. Basbagci, G.; Dolar, F.S. Characterization and pathogenicity of *Rhizoctonia solani* AG-5 isolates obtained from chickpea in Turkey. *J. Phytopathol.* **2022**, *170*, 141–147. [CrossRef]
43. Tanjali, N.; Islam, S.; Akhter, M.S.; Hossain, M.M.; Alam, M.S.; Begum, F. Characterization of *Sclerotium rolfsii* causing foot rot: A severe threat of betel vine cultivation in Bangladesh. *3 Biotech* **2024**, *14*, 58. [CrossRef] [PubMed]
44. Liu, D.Y.; Cheng, H.; Bussmann, R.W.; Guo, Z.Y.; Liu, B.; Long, C.L. An ethnobotanical survey of edible fungi in Chuxiong City, Yunnan, China. *J. Ethnobiol. Ethnomed.* **2018**, *14*, 42. [CrossRef] [PubMed]
45. Guo, J.-W.; Tian, R.-C.; Yang, C.-L.; Jia, L.; Zhou, S.-Y.; Yang, M.; Li, L.; Gao, P.; Yu, L.; Muhammad, M.; et al. The occurrence of *Colletotrichum karstii* and *C. fructicola* causes anthracnose on endangered ethnic vegetable *Yunnanopilia longistaminea* in Yunnan, China. *J. Fungi* **2025**, *11*, 748. [CrossRef] [PubMed]
46. Guo, J.-W.; Yang, C.-L.; Dong, B.-Z.; Tian, R.-C.; Yang, M.; Li, L.; Gao, P.; Zhou, S.-Y.; Muhammad, M.; Bu, Y.; et al. Characterization and biological characteristics of *Alternaria*, *Botryosphaeria*, *Pestalotiopsis*, and *Trichothecium* species associated with postharvest loquat fruit rot in Yunnan, China. *Plants* **2025**, *14*, 3201. [CrossRef] [PubMed]
47. Guo, J.-W.; Yang, H.; Wang, X. Plant functional traits or microbiomes associated with diseases, pests, human activities and climate change. *Plants* **2026**, *15*, 238. [CrossRef] [PubMed]
48. Yang, G.H.; Conner, R.L.; Chen, Y.D. First Report of damping-off of Swiss chard caused by *Rhizoctonia solani* AG4 HG I and binucleate *Rhizoctonia* AGA in China. *Plant Dis.* **2007**, *91*, 1516. [CrossRef] [PubMed]
49. Yang, G.H.; Naito, S.; Dong, W.H. Identification and pathogenicity of *Rhizoctonia* spp. causing wirestem of *Betula nigra* in China. *J. Phytopathol.* **2006**, *154*, 80–83. [CrossRef]
50. Gao, P.H.; Wu, Z.X.; Wei, J.X.; Gao, T.M.; Qi, Y.; Liu, J.N.; Huang, F.Y.; Yu, L. First report of *Athelia rolfsii* associated with southern blight disease of *Amorphophallus muelleri* in China. *Plant Dis.* **2023**, *107*, 3284. [CrossRef]
51. Guo, J.-W.; Yang, L.-F.; Liu, Y.-H.; Yang, J.; Wang, H.-F.; Liu, Y.-H.; Li, W.J. First report of pseudostem black spot caused by *Pestalotiopsis microspora* on tsao-ko in Yunnan, China. *Plant Dis.* **2016**, *100*, 1021. [CrossRef]
52. Hall, T.A. BioEdit: A user-friendly biological sequence alignment editor and analysis program for Windows 95/98/NT. *Nucleic Acids Symp. Ser.* **1999**, *41*, 95–98. [CrossRef]
53. Glez-Peña, D.; Gómez-Blanco, D.; Reboiro-Jato, M.; Fdez-Riverola, F.; Posada, D. ALTER: Program-oriented conversion of DNA and protein alignments. *Nucleic Acids Res.* **2010**, *38*, W14–W18. [CrossRef] [PubMed]
54. Ronquist, F.; Huelsenbeck, J.P. MrBayes 3: Bayesian phylogenetic inference under mixed models. *Bioinformatics* **2003**, *19*, 1572–1574. [CrossRef] [PubMed]
55. Rambaut, A. *FigTree. Tree Figure Drawing Tool*, version 1.4.0; Institute of Evolutionary Biology, University of Edinburgh: Edinburgh, UK, 2012.


**Disclaimer/Publisher's Note:** The statements, opinions and data contained in all publications are solely those of the individual author(s) and contributor(s) and not of MDPI and/or the editor(s). MDPI and/or the editor(s) disclaim responsibility for any injury to people or property resulting from any ideas, methods, instructions or products referred to in the content.